

## Optical-model analysis of two $\rho^0$ -photoproduction experiments\*

Robin Spital and Donald R. Yennie

*Laboratory of Nuclear Studies, Cornell University, Ithaca, New York 14850*

(Received 13 July 1973)

An optical-model analysis of two important experiments measuring  $\rho^0$  photoproduction on complex nuclei is presented. In an effort to determine  $\sigma_\rho$ , the  $\rho^0$ -nucleon total cross section, and  $\alpha_\rho$ , the ratio of the real to the imaginary part of the  $\rho^0$ -nucleon forward elastic scattering amplitude, the best normalization of the theory to the experimental data is determined for many pairs of values of these parameters. It is concluded that uncertainties in the theory make it impossible to determine  $\sigma_\rho$  and  $\alpha_\rho$  uniquely, but that if one is taken as known, the other can be determined well; and the two experiments give approximately the same relationship between  $\sigma_\rho$  and  $\alpha_\rho$ . If  $\alpha_\rho$  is taken to be  $\approx -0.2$ ,  $\sigma_\rho \approx 27$  mb is obtained, consistent with older analyses. Some attention is also focused on  $|f_0|^2$ , the forward differential cross section for  $\rho^0$  photoproduction on one nucleon, and the closely related parameter  $\gamma_\rho^2/4\pi$ . These quantities are somewhat uncertain, however, because of theoretical ambiguities in determining the normalization of the experimental cross sections. Various uncertainties in the optical model are discussed, and it is concluded that they may make small numerical changes in the results but do not affect the qualitative picture.

### I. INTRODUCTION

It is well known that vector mesons play an important part in mediating the hadronic interactions of the photon.<sup>1</sup> Of particular importance are the values of the photon-vector-meson coupling,  $e/f_V$  ( $\equiv e/2\gamma_V$ ), and the vector-meson-nucleon scattering amplitude,  $f_{VV}(\theta)$ . The first gives the amplitude for a real photon to contain a given vector-meson component, and the second is an important ingredient in the theory of the total photon cross section, Compton scattering, and diffractive photoproduction of the vector meson. It is in these diffractive processes that vector-meson dominance (VMD) has been most successful.

Two groups at DESY<sup>2</sup> and Cornell<sup>3</sup> have measured these quantities for the  $\rho^0$  by photoproducing  $\rho^0$ 's on complex nuclei.<sup>4</sup> The great advantage of this method, as first noted by Drell and Trefil<sup>5</sup> and Ross and Stodolsky,<sup>6</sup> is that  $f_{VV}(0)$  can be determined from the dependence of the photoproduction cross section on  $A$ , the number of nucleons in the nucleus, without making use of a particular model, e.g., VMD, to relate  $f_{VV}(0)$  to  $f_{\gamma V}(0)$  (the photoproduction forward amplitude on one nucleon). As we shall see later,  $f_{\gamma V}(0)$  ( $\equiv f_0$ ) enters only the over-all normalization and does not affect the  $A$  dependence.

Those readers familiar with the history of these experiments may recall that several years ago the experimental results from the two groups appeared to be in sharp disagreement. Since that time a more comprehensive DESY-MIT experiment has been carried out and both experiments have been reanalyzed with more realistic models. As shown

in Gottfried's review article,<sup>1</sup> the results of these analyses are now not in disagreement with each other or with other determinations of these parameters. However, the theoretical models employed were not precisely the same. The major purpose of the present work is to treat both sets of data in the same manner, insofar as it is possible to do so. We do not believe that the model used here is necessarily better than the models used by the two experimental groups. However, a secondary purpose of the present work was to gain some knowledge of the sensitivity of the results to various features of the model. This was done in a somewhat cursory fashion, in contrast to the much more thorough work of the DESY group for certain features, such as the nuclear radius. However, the result is that certain combinations of parameters are determined in a way which is rather insensitive to details of the model. Since it is undesirable to compare two experiments only after a lengthy and somewhat complex analysis, we have tried also to compare the data at as primitive a level as possible (it is not possible to compare results at the raw-data level). When this is done, we shall see that these two major experiments appear to agree in the  $\theta=0$  region. However, since there are no Cornell data for finite  $t$ , the final values of the parameters are a bit different.

The paper is organized as follows: Section II contains a concise description of the theoretical model. In Sec. III we present the  $\rho^0$ -photoproduction cross sections ( $d\sigma/dt$ ) which have been extracted from the measured  $\pi\pi$  mass spectra and describe briefly some of the theoretical and prac-

tical uncertainties involved in this step. These uncertainties are discussed in more detail in an accompanying paper.<sup>7</sup> Section IV contains the detailed comparison of theory and experiment, while Sec. V discusses the sensitivity of the results to the theoretical model. In Sec. VI we summarize our conclusions.

## II. THE THEORETICAL MODEL

The theoretical model used is Glauber's<sup>8</sup> optical model of high-energy collisions, suitably generalized to the case of particle production.<sup>5,6,9,10</sup> In this model, the nucleus is pictured as a collection of physical nucleons which are treated as frozen in position during the collision. Nucleons are assumed not to overlap in space, and the incident particle interacts with each nucleon in turn as it passes through the nucleus. These two-body interactions are described by *profile functions*, which are related by Fourier transformation to production or elastic scattering amplitudes. In the case of photoproduction of the  $\rho^0$ , some special features must be noted. One of these is the minimum momentum transfer,  $q_{\parallel}$ , which introduces an additional phase factor that combines with the phase produced by the refractive part of  $f_{\nu\nu}$  (i.e.,  $\text{Re}f_{\nu\nu}$ ) to produce a drastic effect on the over-all production amplitude. This effect, which enhances the sensitivity of the cross section to  $\text{Re}f_{\nu\nu}$  and is extremely important in the energy range of these experiments (5–10 GeV), was first pointed out by Swartz and Talman<sup>11</sup> of the Cornell group.

Another special feature is the instability of the  $\rho^0$ . Since there is no reliable way of using an optical model to predict the  $\pi\pi$  mass spectrum, we attempted to extract from the data the cross section for photoproduction of  $\rho^0$ , as if the  $\rho^0$  were stable. (See Sec. III and Ref. 7 for further discussion of this point.) The optical model was then used to calculate the cross section for stable  $\rho^0$ 's. Throughout our calculations, the value  $m_{\rho} = 770$  MeV was adopted as the standard value until a better value can be obtained from experiment. (Reasons for this choice are discussed in Ref. 7 and briefly in Sec. III.)

The distribution of nuclear matter is treated in the independent-particle approximation corrected for two-body correlations. We took as our input the nuclear-charge distributions. (In principle these are determined by electron scattering. However, we did not make use of the detailed results of electron scattering on each individual nucleus. See Sec. IIC below.) From there, two steps are necessary to determine the "optical" density. One is to unfold the charge density of the protons so as

to obtain the nucleon-number density, under the assumption that neutrons and protons have the same distribution. The second step is to take into account the finite range of the projectile-nucleon interaction by folding it into the nucleon-number density. In contrast, the two experimental groups assumed an optical density directly. The DESY-MIT group adjusted the radius to fit their  $t$  dependence,<sup>12</sup> and the Cornell group made two choices of radius based on other experiments. In retrospect, we do not believe our procedure is significantly more realistic. However, it does show that nuclear radii as determined by electron scattering and by strong interactions are not in disagreement.

The derivation of the optical-model approximation from the multiple-scattering formalism has been presented in several places.<sup>10</sup> Among other things, it involves neglecting terms which appear to be of relative order  $A^{-1}$ . We shall argue in Sec. V that this error is not as important as it might seem in light nuclei, and is in any case intimately tied up with the treatment of correlations.

### A. Coherent photoproduction

The well-known optical-model expression is<sup>5,6</sup>

$$\frac{d\sigma_{\text{coherent}}}{dt}(\gamma A \rightarrow \rho^0 A) = |N_{\text{eff}}(t)|^2 |f_0|^2, \quad (2.1)$$

where

$$N_{\text{eff}}(t) = \int d^2b dz \exp(i\vec{q}_{\perp} \cdot \vec{b} + i q_{\parallel} z) \bar{n}(\vec{b}, z) \times \exp\left(-\frac{1}{2}\sigma_{\rho}(1-i\alpha_{\rho}) \int_z^{\infty} \bar{n}(\vec{b}, z') dz'\right).$$

The physical interpretation of  $N_{\text{eff}}$  is easily read off from this expression. A photon converts to a  $\rho$  meson at  $(\vec{b}, z)$  where  $\vec{b}$  is the impact parameter and  $z$  is the distance along the incident photon direction. The conversion amplitude per nucleon is  $f_0$  (averaged over neutrons and protons),<sup>13</sup> so that

$$\left. \frac{d\sigma}{dt}(\gamma N \rightarrow \rho^0 N) \right|_{\theta=0} = |f_0|^2. \quad (2.2)$$

$\bar{n}$  is the optical density, assumed to be the same for production and subsequent propagation of the  $\rho$  through the nucleus. The transverse momentum transfer is  $\vec{q}_{\perp}$  and the longitudinal is

$$q_{\parallel} = k - (k^2 - m_{\rho}^2)^{1/2} \cong m_{\rho}^2 / 2k, \quad (2.3)$$

where  $k$  is the photon energy (however,  $k$  is not high enough in these experiments to justify this last approximation; use of the approximation can cause errors in heavy nuclei of several percent). In terms of these,  $t = -(\vec{q}_{\perp}^2 + q_{\parallel}^2)$ . The forward  $\rho$

scattering amplitude is

$$f_{\rho\rho} = \frac{ik}{4\pi} \sigma_\rho (1 - i\alpha_\rho) \quad (2.4)$$

(the important parameter  $\alpha_\rho$  is the ratio of the real to the imaginary part of the amplitude). The last exponential corresponds to the absorption and refraction of the  $\rho$  wave after production.

It is assumed that  $\bar{n}$  is known for various nuclei, and that  $|f_0|^2$ ,  $\sigma_\rho$ , and  $\alpha_\rho$  are the experimental parameters to be determined by studying the  $A$  dependence and normalization.

$$\bar{N}_{\text{eff}} = \int d^2b dz \bar{n}(\vec{b}, z) \exp\left(-\sigma_\rho \int_z^\infty \bar{n}(\vec{b}, z') dz'\right) \times \left| 1 - \int_{-\infty}^z dz'' \bar{n}(\vec{b}, z'') \frac{1}{2} \sigma_\rho (1 - i\alpha_\rho) e^{i\alpha_\rho z''} \exp\left(-\frac{1}{2} \sigma_\rho (1 - i\alpha_\rho) \int_{z''}^z \bar{n}(\vec{b}, z''') dz'''\right) \right|^2,$$

where in obtaining (2.5) VMD was used to write  $f_{\gamma\rho} = (e/f_\rho) f_{\rho\rho}$ . Formula (2.5) was used in a very crude way to estimate the effect of incoherent contamination on our analysis—see Sec. IV. It is clearly incorrect at small  $t$  since it fails to take into account the Pauli principle, which suppresses the cross section somewhat in that region.

### C. Specification of the optical density

As mentioned before, the charge density  $n_{\text{ch}}$  is used as an input. However, we did not make a strenuous effort to use realistic charge densities as determined by electron scattering. Instead, for heavy nuclei ( $A > 16$ ), we used a Fermi shape

$$n_{\text{ch}} = n_0 (1 + e^{(r-c)/r_F})^{-1}. \quad (2.6)$$

$z_F$  was kept fixed at 0.545 F for all nuclei and  $c$  was chosen to be 6.6275 F for Pb ( $= 1.12 A_{\text{Pb}}^{1/3}$ ). For all other nuclei,  $c$  was adjusted to give the same central density, as suggested by electron-scattering experiments. Thus  $r_0 \equiv c/A^{1/3}$  varies somewhat with  $A$ , as shown in Table I (see Ref. 14) and in reasonable agreement with electron-scattering determinations as seen there.

The proton charge size was then allowed for (approximately) to obtain a nucleon-number density. This is referred to as unfolding the electromagnetic smearing; the smearing parameter

$$\langle r_{\text{em}}^2 \rangle^{1/2} = 0.8 \text{ F}$$

is the approximate value from  $e-p$  elastic scattering experiments. Next the strong interaction size was folded in to give an optical density. Here we used an interaction radius of

$$\langle r_s^2 \rangle^{1/2} = 0.8 \text{ F},$$

### B. Incoherent $\rho^0$ photoproduction

Equation (2.1) is for coherent  $\rho^0$  photoproduction which naturally dominates at the small  $t$  values of the experimental points [ $-t \leq 0.009$  (GeV/c)<sup>2</sup>].

There is always, however, contamination from incoherent production. The optical-model result for incoherent  $\rho$  photoproduction is<sup>9</sup>

$$\frac{d\sigma_{\text{incoherent}}}{dt}(\gamma A \rightarrow \rho^0 A) = \bar{N}_{\text{eff}} \frac{d\sigma}{dt}(\gamma N \rightarrow \rho^0 N), \quad (2.5)$$

with

corresponding to a slope parameter  $b$  (in  $d\sigma/dt \propto e^{bt}$ ) of 8 GeV<sup>-2</sup> in the two-body scattering. This is a reasonable number for the type of reactions we are considering here. It might appear that the two smearings would exactly compensate. However, this is not the case since the charge folding is three-dimensional and the strong folding is two-

TABLE I. Values of  $r_0 \equiv c/A^{1/3}$  for our model and from electron scattering. We selected  $r_0(\text{Pb}) = 1.12$  by matching a Fermi density to the skin region of the very accurate charge-density determination of J. Heisenberg *et al.*,<sup>14</sup> which includes both electron and muon scattering data. Incidentally, the corresponding root-mean-square radius, 5.49 F, agrees excellently with the measured root-mean-square radius of Heisenberg *et al.*

Element	$A^a$	Our $r_0^b$	Electron scattering $r_0^c$
U	238.1	1.122	...
Pb	207.2	1.12	1.09
Au	197.0	1.119	1.10
W	183.9	1.118	...
Ta	181.0	1.118	1.13
In	114.7	1.108	1.08
Cd	112.4	1.108	...
Ag	107.9	1.107	...
Cu	63.5	1.091	...
Ti	47.9	1.080	1.03 <sup>d</sup>
Al	27.0	1.048	1.02

<sup>a</sup> These values of  $A$  were taken from Ref. 2 in order to help minimize the difference between our model and that of DESY-MIT.

<sup>b</sup> The quantity given is  $c/A^{1/3}$ .

<sup>c</sup> Taken from R. Hofstadter and H. R. Collard, in *Landolt-Börnstein* (Springer, Berlin, 1967), Group 1, Vol. 2.

<sup>d</sup> Interpolated between Ti<sup>46</sup> and Ti<sup>50</sup> in the reference of note c.

dimensional (transverse to the incident momentum). The resulting density is called  $\tilde{n}(\vec{b}, z)$ , normalized so that  $\int \tilde{n}(\vec{b}, z) d^2b dz = A$ .

The correlations between nucleons have been included by introducing an effective correlation length of 0.3 F (Ref. 15) at the center of the nucleus. This agrees with Moniz and Nixon,<sup>10</sup> but is a factor of 2 smaller than the value suggested by von Bochmann, Margolis, and Tang (BMT)<sup>16</sup> and used in the DESY-MIT analysis. We cannot account for this difference since BMT do not give the correlation function from which their value was derived. For want of a better theory, this correlation length is allowed to vary like  $\tilde{n}^{-1/3}$  throughout the nucleus; this is the variation which would come from the exclusion principle alone. Thus  $\tilde{n}$  was everywhere replaced by

$$\tilde{n} \left\{ 1 + \frac{1}{2} l_c \sigma_\rho \tilde{n} \left[ \frac{\tilde{n}(r=0)}{\tilde{n}} \right]^{1/3} \right\}.$$

It seems to us that the treatment of correlations is one of the most deficient aspects of the model. However, the effect of correlations is small; so even an error comparable to the effect is not too serious. This is one of the intangible sources of theoretical error in the model.

For  $A \leq 16$ , we used a shell-model charge density of the form

$$\rho = \rho_0 \left( 1 + \delta \frac{r^2}{a_0^2} \right) e^{-r^2/a_0^2},$$

where  $\delta$  was not restricted to the shell-model value  $[\frac{1}{8}(A-4)]$  but was taken from electron scattering. The values of the parameters actually used are given in Table II. The smearing and correlations were treated as with the heavy nuclei, with  $l_c$  normalized to 0.3 F at the central density of the heavy nuclei. We will return to discuss the effect of small changes in these assumptions in Sec. V.

### III. PRELIMINARY ANALYSIS OF THE DATA TO DETERMINE $d\sigma/dt$

The experimental data consist of values of  $d\sigma/dt dm_{\pi\pi}$  averaged over some experimental aperture. There exists no good theory for this double differential cross section although there is a good qualitative understanding of the main features of the  $m_{\pi\pi}$  dependence. The optical model of Sec. II treats the  $\rho$  as stable, so we have the choice of either adapting the data to that model or generalizing the model to the production of a mass spectrum. Some of the difficulties of the latter approach are discussed in the accompanying paper.<sup>7</sup> The main complication is the nonresonant pion-pair (Drell) amplitude, which interferes with the

TABLE II. Light-element nuclear parameters taken from electron scattering.

Element	A	$a_0$	$\delta$
C <sup>a</sup>	12	1.649	1.25
Be <sup>b</sup>	9	1.71	0.833

<sup>a</sup> Taken from I. Sick and J. S. McCarthy, Nucl. Phys. A150, 631 (1970).

<sup>b</sup> Taken from reference of note c, Table I.

diffractive  $\rho$  amplitude. In addition, there are specifically nuclear effects, as treated by Gottfried and Julius<sup>17</sup> and Bauer.<sup>18</sup> It is our opinion that the theory is too unreliable to attempt a detailed explanation of the mass spectrum.

Instead, we try to find from the experimental data the cross section a stable  $\rho^0$  would have. By this we mean the cross section which would result if the interaction producing the decay were turned off, but with the  $\rho^0$  otherwise interacting strongly. This is necessarily an approximate concept, but we feel that it is physically the most reasonable approach. Since the production amplitude for the decaying  $\rho^0$  varies in an unknown way as a function of the pair mass, we define the cross section in terms of the production amplitude at the  $\rho$  mass. There are arguments that the interfering Drell amplitude is precisely canceled at the  $\rho$  mass.<sup>18,19</sup> It is also our opinion that it is not possible to make a unique background subtraction for nonresonant noninterfering pion pairs. In fitting the mass distributions, we do not find it necessary to introduce such a background, but there could certainly be a contamination of this sort in the data. We choose simply to ignore the presence of such a background, therefore possibly overestimating the cross section slightly. With these assumptions, the differential cross section is defined by

$$\frac{d\sigma}{dt} \equiv \frac{\pi\Gamma_\rho}{2} \frac{d\sigma}{dt dm_{\pi\pi}} \Big|_{m=m_\rho} \quad (3.1)$$

This definition is to be contrasted with the "area" method in which one integrates  $d\sigma/dt dm_{\pi\pi}$  with respect to  $m_{\pi\pi}$ . The area method suffers from the defect that it is difficult (i.e., impossible) to tell how much of the area is to be attributed to the  $\rho$  meson. That is, it depends on the unknown dependence of the production amplitude with mass.

Unfortunately, even if (3.1) is accepted as a good definition, there remain some practical difficulties. The parameters  $\Gamma_\rho$  and  $m_\rho$  are not precisely known; in fact,  $\Gamma_\rho$  is quite poorly known. The difficulty in determining the parameters from photoproduction experiments is discussed in the accompanying paper<sup>7</sup>; it is of course related to the

inadequate theory of the mass distribution. Therefore we have arbitrarily chosen standard values of these parameters, pending a better determination from some other type of experiment. The standard values used in the data analysis are

$$m_{\rho}^{\text{std}} = 770 \text{ MeV}, \quad \Gamma_{\rho}^{\text{std}} = 127 \text{ MeV}. \quad (3.2)$$

This choice has no particular significance; it just represents some of our former prejudices. This standard definition has two advantages:

(1) It makes comparison easy between almost all types of experiments and, more importantly,

(2) *the cross sections so obtained are nearly exactly proportional to the assumed value of  $\Gamma_{\rho}$ .*

Because of (2) above,  $\sigma_{\rho}$  and  $\alpha_{\rho}$  can be deduced from the  $A$  dependence of the cross sections independently of the assumed value of  $\Gamma_{\rho}$ . In addition, the values of  $\gamma_{\rho}^2/4\pi$  and  $|f_0|^2$  can be trivially corrected for different assumed widths. As the reader will discover in Ref. 7, the values of  $m_{\rho}$  and  $\Gamma_{\rho}$  obtained from fitting the high-resolution  $\rho$ - $\omega$  interference data of the DESY-MIT group<sup>20</sup> depend greatly on the particular mass distribution being fitted and we can see no way at present of determining these numbers convincingly.

To apply (3.1) to the data, we now fit a theoretical curve to  $d\sigma/dt \, dm_{\pi\pi}$  and read off the value at  $m_{\rho}$ .

However, it is immediately clear that there exists the danger that imposing (3.2) directly could lead to a serious error. For example, if the experimental mass determination is systematically wrong by 1%, the right-hand side of (3.1) will be evaluated at the wrong point (777 or 763 MeV) on a curve falling rapidly with increasing  $m_{\pi\pi}$ . Therefore the best value of  $m_{\rho}$  was determined for each experiment by a fit to the entire data matrix of that experiment. Thus each experiment was allowed to "choose" its own  $\rho^0$  mass. The mass so chosen was thereafter held fixed in the fits made to the individual mass spectra.

The Cornell experimental data were already treated by essentially the method described above, so our analysis starts with the values of  $d\sigma/dt$  provided by them but adjusted in two ways: (i) Their cross sections were interpolated between their assumed nuclear radii to the radii used by us. (Since their data came from a finite aperture, it was necessary for them to assume a  $t$  dependence in order to determine the  $\theta=0$  cross section. They used an optical model with two different assumptions for the nuclear radius to calculate this  $t$  dependence.) (ii) Their cross sections were adjusted by the factor  $127/124$  to take into account the differences in assumed widths. We note that the best value of  $m_{\rho}$  for their data is 775 MeV. Our version of their cross sections is given in Table III.

The DESY-MIT group provides complete tables

of  $(1/A)d\sigma/d\Omega \, dm_{\pi\pi}$  for 13 values of  $A$ , 3 values of  $k$ , 5 values of  $t$ , and 18 values of  $m_{\pi\pi}$ . In extracting the cross sections given in Table IV, we used only the nine central data points from each spectrum (675 to 885 MeV in steps of 30 MeV) to minimize the effects of the extremes of the mass spectra where both theory and experiment are most uncertain. In each individual fit the mass was kept fixed at 770 MeV, in accordance with an over-all fit made to the entire data matrix. The width was fixed at 127 MeV and the cross section determined by (3.2).

The cross sections given in the tables include both coherent and incoherent  $\rho$  photoproduction. The experiments cannot distinguish between these two processes. The effect of the incoherent production will be taken into account, albeit rather crudely, in Sec. IV.

#### IV. COMPARISON OF THEORY AND EXPERIMENT

We turn now to the comparison of the cross sections given in Tables III and IV of Sec. III with the theoretical model of Sec. II. Our main concern is  $\sigma_{\rho}$  and  $\alpha_{\rho}$ . As a byproduct of the analysis we also obtain values of  $\gamma_{\rho}^2/4\pi$  and  $|f_0|^2$ ; but these are less significant since they depend on the choice of  $\Gamma_{\rho}$ . When a better theory dispels the mist surrounding  $\Gamma_{\rho}$ , however, our results can be trivially adjusted for the correct width as noted in Sec. III.

Figure 1 illustrates our analysis procedure schematically. We have already described the extraction of experimental values of  $d\sigma/dt(\gamma A \rightarrow \rho^0 A)$  in Sec. III and now proceed to discuss the other steps in detail.

For each experimental measurement of  $d\sigma/dt(\gamma A \rightarrow \rho^0 A)$  optical-model calculations were made for  $\sigma_{\rho} = 21, 22, \dots, 37$  mb and  $-\alpha_{\rho}$  of 0, 0.05, 0.1,  $\dots$ , 0.45 (except that for  $\sigma_{\rho N} > 30$  mb, the high-

TABLE III. Our version of the Cornell forward cross sections (mb/GeV<sup>2</sup>). The numbers of Ref. 3 have been raised by a factor  $\frac{127}{124}$ , and radius interpolations have been made. See the text for details.

Element	$\left. \frac{d\sigma}{dt}(\gamma A \rightarrow \rho^0 A) \right _{\theta=0}$			
	$k$	6.1 GeV	6.5 GeV	8.8 GeV
D		0.413 ± 0.017	0.449 ± 0.018	0.371 ± 0.011
Be		5.87 ± 0.17	...	5.62 ± 0.13
C		9.91 ± 0.28	9.00 ± 0.28	9.15 ± 0.15
Mg		31.1 ± 0.9	32.3 ± 1.2	32.6 ± 0.8
Cu		135 ± 4	125 ± 4	136 ± 3
Ag		279 ± 9	270 ± 9	303 ± 7
In		...	...	348 ± 9
Au		549 ± 16	...	707 ± 17
Pb		584 ± 18	638 ± 26	789 ± 22

TABLE IV. Results of our mass fits to DESY-MIT data of Ref. 2. The prescription of Sec. III is applied to obtain  $d\sigma/dt$  (mb/GeV<sup>2</sup>).

$\frac{d\sigma}{dt} (\gamma A \rightarrow \rho^0 A)$				$\frac{d\sigma}{dt} (\gamma A \rightarrow \rho^0 A)$					
A	$\frac{-t}{(\text{GeV}^2)} \setminus \frac{k}{(\text{GeV})}$	5.8	6.2	6.6	A	$\frac{-t}{(\text{GeV}^2)} \setminus \frac{k}{(\text{GeV})}$	5.8	6.2	6.6
U <sup>238</sup>	0.001	412 ± 14.7	475 ± 13.5	496 ± 13.3	Al <sup>27</sup>	0.001	30.1 ± 1.2	31.1 ± 0.96	29.9 ± 1.0
	0.003	184 ± 16.4	209 ± 13.3	223 ± 13.1		0.003	23.2 ± 1.8	25.3 ± 1.3	22.8 ± 1.3
	0.005	83.7 ± 13.9	91.3 ± 11.4	78.6 ± 10.9		0.005	25.0 ± 2.1	21.3 ± 1.5	18.3 ± 1.6
	0.007	50.2 ± 12.3	25.1 ± 7.0	26.0 ± 7.4		0.007	16.4 ± 2.4	19.0 ± 1.5	17.8 ± 1.7
	0.009	30.0 ± 9.6	9.3 ± 4.5	9.4 ± 2.8		0.009	17.5 ± 2.5	15.3 ± 1.5	14.6 ± 1.6
Pb <sup>207</sup>	0.001	388 ± 15.3	438 ± 13.3	438 ± 12.7	C <sup>12</sup>	0.001	8.54 ± 0.33	8.85 ± 0.27	8.28 ± 0.28
	0.003	159 ± 17.6	202 ± 13.9	215 ± 13.3		0.003	7.53 ± 0.51	7.80 ± 0.38	7.65 ± 0.39
	0.005	63.3 ± 14.6	72.5 ± 12.2	78.9 ± 11.2		0.005	6.62 ± 0.60	6.77 ± 0.47	6.48 ± 0.47
	0.007	40.7 ± 14.6	30.8 ± 8.6	27.8 ± 9.1		0.007	5.01 ± 0.72	5.78 ± 0.48	5.78 ± 0.50
	0.009	29.5 ± 12.3	7.2 ± 5.1	12.3 ± 4.2		0.009	4.84 ± 0.71	5.68 ± 0.45	5.34 ± 0.48
Au <sup>197</sup>	0.001	358 ± 17.8	412 ± 14.6	416 ± 13.8	Be <sup>9</sup>	0.001	5.08 ± 0.22	5.48 ± 0.18	5.35 ± 0.20
	0.003	164 ± 20.1	210 ± 16.4	191 ± 13.9		0.003	4.23 ± 0.33	5.28 ± 0.27	4.77 ± 0.27
	0.005	102 ± 19.2	86.5 ± 14.3	82.0 ± 12.7		0.005	3.18 ± 0.36	3.97 ± 0.31	4.47 ± 0.33
	0.007	36.6 ± 15.8	49.6 ± 10.9	37.9 ± 11.0		0.007	3.46 ± 0.47	3.96 ± 0.34	3.59 ± 0.33
	0.009	23.2 ± 12.6	11.1 ± 6.3	15.2 ± 5.6		0.009	3.39 ± 0.52	3.80 ± 0.33	3.26 ± 0.34
W <sup>183</sup>	0.001	337 ± 15.9	374 ± 13.2	391 ± 13.8	Ag <sup>108</sup>	0.001	192 ± 7.0	203 ± 6.0	207 ± 5.8
	0.003	156 ± 18.7	193 ± 15.4	224 ± 15.0		0.003	110 ± 8.6	129 ± 6.9	137 ± 6.8
	0.005	79.8 ± 17.5	78.3 ± 13.4	114 ± 13.9		0.005	67.6 ± 8.2	86.5 ± 7.1	70.1 ± 6.6
	0.007	41.0 ± 16.0	46.7 ± 10.9	13.8 ± 11.6		0.007	34.0 ± 8.3	41.2 ± 5.5	46.4 ± 5.9
	0.009	29.2 ± 12.4	10.6 ± 7.6	22.7 ± 6.6		0.009	17.0 ± 6.8	32.0 ± 4.9	23.5 ± 4.4
Ta <sup>181</sup>	0.001	328 ± 12.3	350 ± 11.5	393 ± 11.4	Cu <sup>64</sup>	0.001	109 ± 4.3	5.48 ± 0.18	108 ± 3.5
	0.003	171 ± 14.1	164 ± 11.1	201 ± 12.0		0.003	65.5 ± 5.7	5.28 ± 0.27	77.0 ± 4.2
	0.005	88.6 ± 12.7	92.4 ± 10.8	102 ± 10.8		0.005	61.1 ± 6.5	3.97 ± 0.31	53.8 ± 4.6
	0.007	41.5 ± 12.8	31.4 ± 7.3	36.1 ± 8.04		0.007	32.7 ± 6.5	3.96 ± 0.34	39.5 ± 4.5
	0.009	14.1 ± 7.1	18.4 ± 5.2	13.3 ± 4.4		0.009	16.8 ± 6.0	3.80 ± 0.33	35.4 ± 4.4
In <sup>115</sup>	0.001	217 ± 8.5	234 ± 7.1	235 ± 7.4	Ti <sup>48</sup>	0.001	71.8 ± 3.2	8.85 ± 0.27	75.7 ± 2.7
	0.003	121 ± 10.3	139 ± 8.5	157 ± 8.4		0.003	50.3 ± 4.3	7.80 ± 0.38	58.3 ± 3.4
	0.005	89.8 ± 11.0	83.7 ± 8.7	72.7 ± 7.7		0.005	43.5 ± 4.9	6.77 ± 0.47	39.1 ± 3.7
	0.007	37.1 ± 9.8	49.9 ± 6.9	39.2 ± 7.0		0.007	26.1 ± 5.2	5.78 ± 0.48	30.7 ± 3.9
	0.009	28.4 ± 8.9	14.2 ± 4.8	28.7 ± 5.8		0.009	14.1 ± 4.6	5.68 ± 0.45	22.2 ± 3.3
Cd <sup>112</sup>	0.001	204 ± 9.0	227 ± 7.4	235 ± 7.3					
	0.003	119 ± 10.7	136 ± 8.8	132 ± 8.1					
	0.005	72.8 ± 11.0	81.0 ± 9.1	78.9 ± 8.5					
	0.007	34.5 ± 10.3	45.9 ± 7.7	37.0 ± 7.6					
	0.009	16.5 ± 8.7	26.1 ± 6.2	32.7 ± 6.2					

est value of  $-\alpha_\rho$  was 0.25 or 0.3). In all these calculations  $m_\rho$  was kept at 770 MeV, and the nuclear models were as described in Sec. II. This produced a large matrix of cross sections dependent on  $A$ , energy,  $t$ ,  $\sigma_\rho$ , and  $\alpha_\rho$ . For each energy,  $\sigma_\rho$ , and  $\alpha_\rho$ , the over-all normalization of the theory (i.e.,  $|f_0|^2$ ) to the experimental data was varied to minimize  $\chi^2$ ; the data from the two different experiments were treated separately. This determination then gave a value of  $\chi^2$  for each  $\sigma_\rho$  and  $\alpha_\rho$  at each energy as well as values of  $\gamma_\rho^2/4\pi$  and  $|f_0|^2$ .  $\chi^2$  maps from these tables are shown in Figs. 2 and 3.

All the results have a few outstanding common

features:  $\chi^2$  is extremely flat along a "valley" in these maps, indicating that acceptable fits to the data can be achieved for any reasonable value of  $\sigma_\rho$  by appropriate choice of  $\alpha_\rho$ . High values of  $\sigma_\rho$  (32 to 34 mb) go with  $\alpha_\rho = 0$  while small values of  $\sigma_\rho$  (~22 mb) go with large real parts.

Before going on to specific details, the question of absolute minima in the  $\chi^2$  valleys at once arises. How should these be interpreted? It is our opinion that the position of these minima cannot be taken seriously. The precise positions are highly sensitive to small variations in the  $A$  dependence of the optical model. Such variations can arise from uncertainties in the theoretical model or in

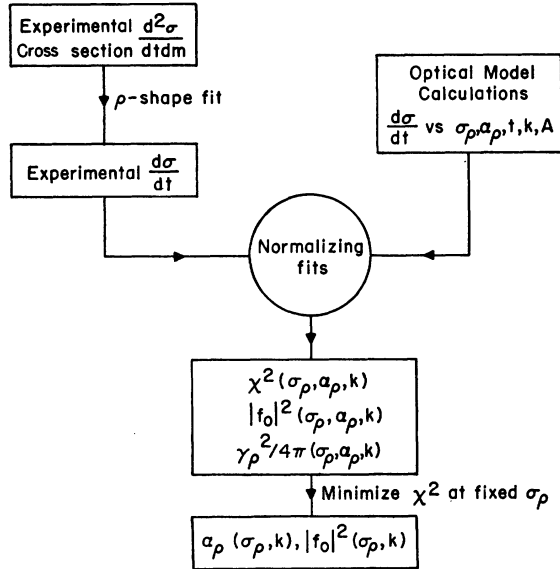
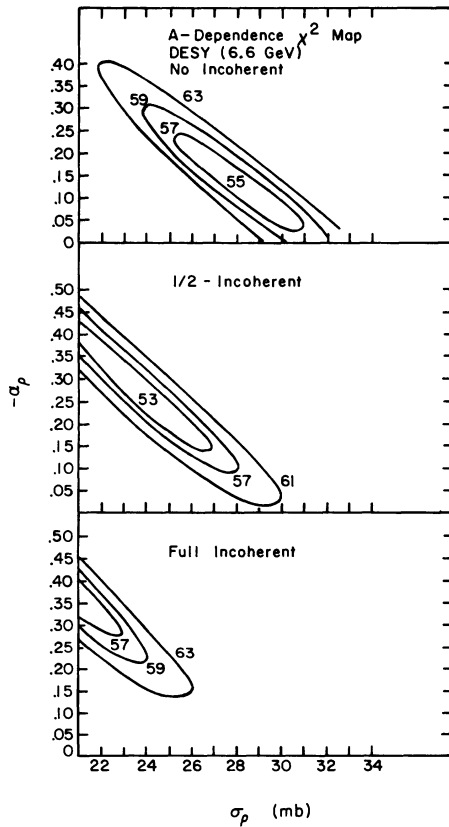
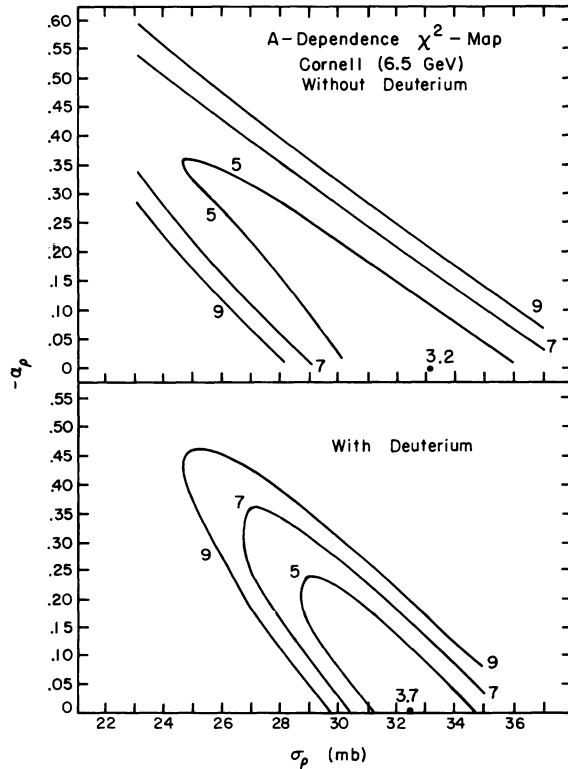


FIG. 1. Schematic outline of the analysis procedure.

FIG. 2.  $\chi^2$ -contour maps for the DESY-MIT 6.6-GeV data using various assumptions for incoherent contamination explained in the text. The number of degrees of freedom, hereafter denoted by  $\langle \chi^2 \rangle$ , is 62.

the mass of the  $\rho^0$ , as will be discussed in Sec. V. We also note that in the case of the Cornell A-dependence fits (Table V), taking the minima positions literally would force one to accept an unreasonably rapid energy variation of  $\sigma_\rho$  and  $\alpha_\rho$ .

In addition, there is the contribution of incoherent  $\rho$  photoproduction which we have not attempted to calculate precisely. Although a more sophisticated treatment of that problem has been given by Trefil,<sup>21</sup> for our purposes it was deemed sufficient to use our general incoherent-processes program to get a rough estimate of the effect. Since this program ignores the Pauli principle which suppresses the incoherent cross section at small  $t$ , it gives an overestimate of the correction needed. (We call the incoherent cross section thus calculated "full-strength" incoherent.) Figure 2 shows  $\chi^2$  maps for the 6.6-GeV DESY-MIT data for various "incoherent corrections" to the experimental data. As can be seen, the position of the minimum changes with the strength of the correction and, generally speaking, the valley is displaced parallel to itself toward lower values of  $\alpha_\rho$  as the strength is increased. Half-strength gives a significant lowering of  $\chi^2$  indicating the

FIG. 3.  $\chi^2$  maps for the Cornell 6.5-GeV data with the deuteron omitted/included.  $\langle \chi^2 \rangle = 3$  with the deuteron, 2 without.

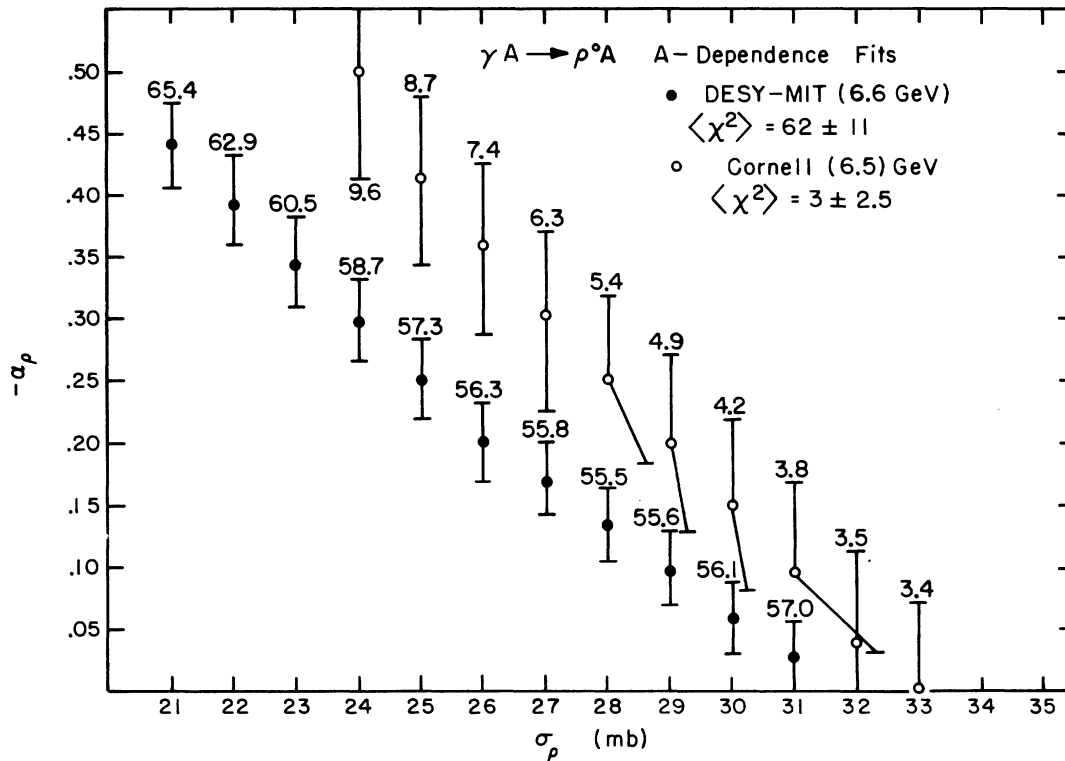


FIG. 4. The curves  $\alpha_\rho(\sigma_\rho)$  for Cornell (DESY-MIT) at 6.5 (6.6) GeV. The "error" on  $\langle \chi^2 \rangle$  is  $(2\langle \chi^2 \rangle)^{1/2}$ .

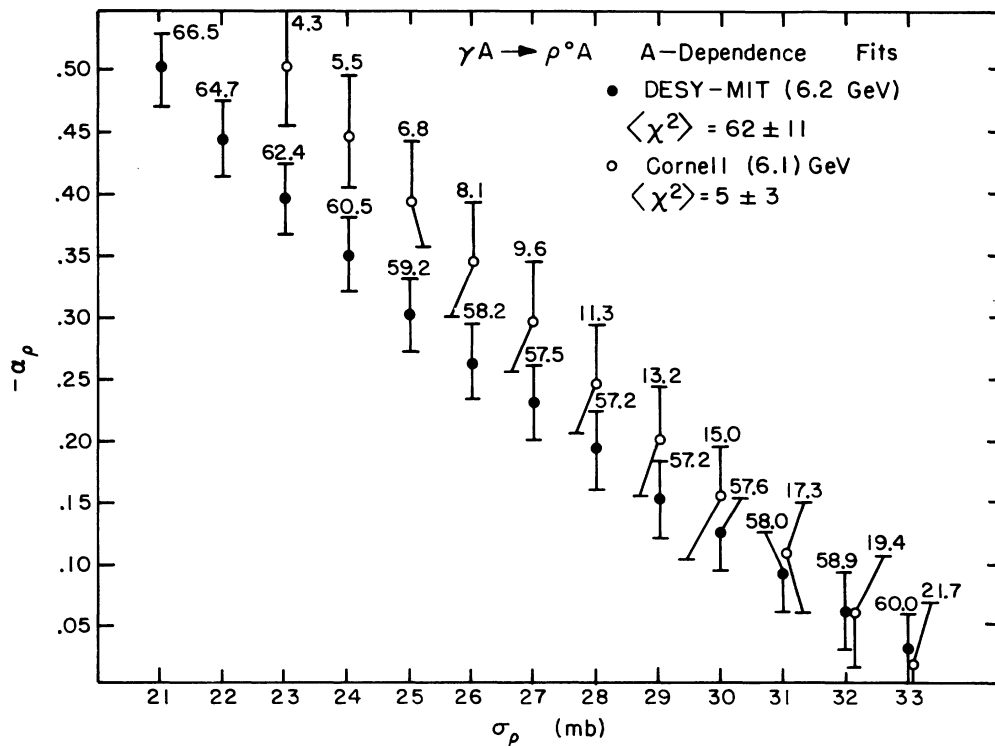


FIG. 5. The curves  $\alpha_\rho(\sigma_\rho)$  for Cornell (DESY-MIT) at 6.1 (6.2) GeV. The "error" on  $\langle \chi^2 \rangle$  is  $(2\langle \chi^2 \rangle)^{1/2}$ .



presence of some incoherent  $\rho$ . For simplicity, however, the rest of our discussion will refer to  $A$ -dependence fits made with no "incoherent corrections." (See Sec. V for further discussion of this point.)

Taking these model uncertainties into account, it is best to regard the data as providing a functional relationship between  $\alpha_\rho$  and  $\sigma_\rho$ . We may then take either of these as the independent variable and use the data to determine the best value of the other.

Choosing to keep  $\sigma_\rho$  fixed, we proceed as indicated in the lower part of Fig. 1. The best value of  $\alpha_\rho$  for fixed  $\sigma_\rho$  (at a given energy) was found by fitting a quadratic function to the  $\sigma_\rho$  column of the appropriate  $\chi^2$  table. Some of the results  $\alpha_\rho(\sigma_\rho, k)$  are shown in Figs. 4 and 5 and are given in Tables V and VI. Those tables also give the  $\chi^2$  for the best fit as well as values of  $|f_0|^2(\sigma_\rho, k)$  and  $(\gamma_\rho^2/4\pi)(\sigma_\rho, k)$ , which were determined by interpolation. The fitting errors of these latter two quantities are quite small, and are unimportant compared to their uncertainty due to  $\Gamma_\rho$ . Typical fitting errors for  $\gamma_\rho^2/4\pi$  ( $|f_0|^2$ ) are 2 to 4% for Cornell and 2 to 3% for DESY-MIT.

The DESY-MIT group measured the  $\pi\pi$  mass spectrum at 5 different values of  $-t$  (0.001, 0.003, 0.005, 0.007, 0.009 GeV<sup>2</sup>) while the Cornell group measured only forward photoproduction (using an optical model similar to our own for a final extrapolation to  $\theta=0$ ). The DESY-MIT group, therefore, had much better statistics and if one were to take the positions of  $\chi^2$ -map minima seriously, the DESY-MIT experiment would give smaller errors. One might also hope that the unreasonably rapid energy variation of the Cornell minima (see Table V) would be removed by more data. Furthermore, our fits to the Cornell 8.8-GeV data have a rather large  $\chi^2$  (15 for 6 degrees of freedom) and there is a possibility that more data would improve some suspicious points that are giving us trouble. However, there is no reason to suspect this is other than a bad statistical fluctuation.

Nevertheless, for reasons mentioned above, the precise positions of  $\chi^2$ -map minima must be largely disregarded. Also, what the Cornell group lost in statistics, it largely made up through its measurements on the deuteron—a target not used by DESY. The cross section for  $D$  is given approximately by  $d\sigma/dt|_{\theta=0}(\gamma D \rightarrow \rho^0 D) \approx 4|f_0|^2$ . The Glauber correction to this process is only about 7% and it is only in the Glauber correction that  $\sigma_\rho$  and  $\alpha_\rho$  enter. Hence the deuteron is much more sensitive to the normalization than to  $\sigma_\rho$  and  $\alpha_\rho$  and its presence serves to tie down the normalization in the  $A$ -dependence fitting. The presence of the deuteron thus results in a sharpening of the

$\chi^2$ -map valleys as well as a better determination of  $|f_0|^2$ . In fact, a glance at the  $\chi^2$  maps of Figs. 2 and 3 reveals that the Cornell maps are much sharper than would be expected from the ratio of the number of degrees of freedom: DESY-MIT (6.6) / Cornell (6.5) =  $\frac{82}{3}$ . As Fig. 3 (a) shows, removal of the deuteron enormously broadens the valley. (Without deuterium the  $\chi^2$  map is essentially flat at  $\chi^2=3.5$  to 4.5 from  $\sigma_{\rho N}=27$  mb on out, but with deuterium the minimum of the Cornell data is  $\sigma_{\rho N}=31\text{mb} \pm 3$  mb.) We also note that with the deuteron the Cornell values of  $|f_0|^2$  vary from 115 to 126  $\mu\text{b}/\text{GeV}^2$  while without the deuteron the range is 109 to 126 (here  $\sigma_{\rho N}$  goes from 23 to 33 mb). In the same range of  $\sigma_{\rho N}$  the DESY-MIT data yield  $|f_0|^2$  from 103 to 122  $\mu\text{b}/\text{GeV}^2$ . Similar results hold for a comparison of the two groups at 6.1 and 6.2 GeV as can be seen from Tables V and VI.

Figure 6 shows the possible effect of a measurement of deuteron  $\rho^0$ -photoproduction on the DESY-MIT 6.6-GeV  $A$ -dependence fit. For this purpose hypothetical deuterium data were constructed using a given fraction of the Cornell value at 6.5 GeV for the normalization and a  $t$  dependence based on deuteron form factors supplied to us by Schumacher.<sup>22</sup> Plotted in the figure are the minima positions and error ellipses ( $\chi^2_{\text{min}}+1$  contours) as a function of the normalization assumed. As can be seen, the size of the error ellipse is considerably reduced when the deuteron is included. Furthermore, it would appear that Cornell's 6.5-GeV deuteron-photoproduction cross section is quite consistent with the DESY 6.6-GeV data.

Figure 7 shows the effect of fitting only  $t = -0.001$  GeV<sup>2</sup> DESY-MIT data. As can be seen, the position of the DESY minima is largely unaffected but the  $\chi^2$  valley is now enormously broad and flat as one would expect. In fact the valley now has the same general character as the Cornell  $\chi^2$  maps for the no-deuterium case. Note that even with  $\frac{2}{3}$  of its data omitted, the DESY-MIT group still has 10 degrees of freedom compared to only 3 for Cornell. Yet the Cornell  $\chi^2$  map [Fig. 3(b)] is much sharper than the map of Fig. 7. It is therefore clear that a great deal is gained by the Cornell group from their deuteron measurements.

The  $\alpha_\rho$  vs  $\sigma_\rho$  curves shown in Figs. 4 and 5 require some comment. These are nearly linear (for fixed  $k$ ) with slopes of roughly 0.05/mb; the absolute value of this slope decreases very slowly as  $\sigma_\rho$  is increased. The Cornell curves have a somewhat sharper slope than the DESY-MIT curves and there is an apparent disagreement at the smaller values of  $\sigma_\rho$ . This may seem rather surprising in view of the fact that the comparisons of

TABLE V. Cornell  $A$ -dependence fits at fixed  $\sigma_\rho$ .

$\sigma_\rho$ (mb)	23	24	25	26	27	28
$k = 6.1$ GeV						
$-\alpha_\rho$	$0.51 \pm 0.05$	$0.45 \pm 0.04$	$0.39 \pm 0.04$	$0.34 \pm 0.04$	$0.29 \pm 0.04$	$0.24 \pm 0.04$
$\chi^2_\rho$	4.3	5.5	6.8	8.1	9.6	11.3
$ f_0 ^2$ ( $\mu\text{b}/\text{GeV}^2$ )	118	119	120	122	123	124
$\gamma_\rho^2/4\pi$	0.52	0.54	0.56	0.58	0.60	0.62
$k = 6.5$ GeV						
$-\alpha_\rho$	$0.57 \pm 0.08$	$0.51 \pm 0.08$	$0.42 \pm 0.07$	$0.36 \pm 0.07$	$0.31 \pm 0.07$	$0.25 \pm 0.07$
$\chi^2_\rho$	11.4	9.6	8.6	7.4	6.3	5.4
$ f_0 ^2$ ( $\mu\text{b}/\text{GeV}^2$ )	115	117	117	118	119	120
$\gamma_\rho^2/4\pi$	0.56	0.58	0.59	0.61	0.62	0.65
$k = 8.8$ GeV						
$-\alpha_\rho$	$0.44 \pm 0.04$	$0.36 \pm 0.04$	$0.29 \pm 0.04$	$0.21 \pm 0.05$	$0.14 \pm 0.05$	$0.066 \pm 0.05$
$\chi^2_\rho$	14.7	15.0	16.0	17.2	18.8	20.5
$ f_0 ^2$ ( $\mu\text{b}/\text{GeV}^2$ )	103	104	105	106	107	108
$\gamma_\rho^2/4\pi$	0.57	0.58	0.60	0.62	0.65	0.68
$\sigma_\rho$ (mb)	29	30	31	32	33	
$k = 6.1$ GeV						
$-\alpha_\rho$	$0.20 \pm 0.04$	$0.15 \pm 0.04$	$0.11 \pm 0.05$	$0.061 \pm 0.05$	$0.018 \pm 0.05$	
$\chi^2_\rho$	13.2	15.0	17.3	19.4	21.7	
$ f_0 ^2$ ( $\mu\text{b}/\text{GeV}^2$ )	125	127	128	129	130	
$\gamma_\rho^2/4\pi$	0.65	0.68	0.71	0.74	0.78	
$k = 6.5$ GeV						
$-\alpha_\rho$	$0.20 \pm 0.07$	$0.15 \pm 0.07$	$0.097 \pm 0.07$	$0.043 \pm 0.08$	$-0.005 \pm 0.07$	
$\chi^2_\rho$	4.8	4.2	3.8	3.5	3.4	
$ f_0 ^2$ ( $\mu\text{b}/\text{GeV}^2$ )	121	123	124	125	126	
$\gamma_\rho^2/4\pi$	0.67	0.70	0.73	0.77	0.81	
$k = 8.8$ GeV						
$-\alpha_\rho$	$-0.003 \pm 0.05$	$-0.1 \pm 0.05$				
$\chi^2_\rho$	23.0	24.9				
$ f_0 ^2$ ( $\mu\text{b}/\text{GeV}^2$ )	110	112				
$\gamma_\rho^2/4\pi$	0.71	0.76				

the  $\theta=0$  data at Cornell (DESY-MIT) 6.5 (6.6) and 6.1 (6.2) GeV show that except for the case of Al (DESY-MIT) and Mg (Cornell), there is excellent agreement between the two experiments (see Fig. 8). It must be borne in mind, however, that the curves of Figs. 4 and 5 include the DESY-MIT  $t$  dependence and the Cornell deuterium measurements. If one compares DESY-MIT ( $t = -0.001$ )-only curves with Cornell no-deuterium curves, the agreement between the two groups expected from the  $\theta=0$  data comparison is realized. In any event this disagreement disappears for  $\sigma \geq 28$  mb. The values of  $\gamma_\rho^2/4\pi$  obtained from the fits are in excellent agreement between the two groups.

Tables V and VI give results for fixed values of  $\sigma_\rho$ . Since the analyses of the two groups themselves were done with  $\alpha_\rho$  fixed, we have also done an analysis with fixed  $\alpha_\rho$  and give some of our results for this method in Tables VII and VIII. We

agree well with the older analyses.

We summarize our conclusions:

(a) The theory is not sufficiently well understood to enable one to extract  $\sigma_\rho$  and  $\alpha_\rho$  from these experiments. If, however, one takes  $-\alpha_\rho = 0.2$  as suggested by Compton scattering<sup>23</sup> and/or observations of electron-pair decays of  $\rho^0$ 's photoproduced on light nuclei,<sup>24</sup> Tables VII and VIII give  $\sigma_\rho = 27.1 \pm 0.3$  mb, which is consistent with Anderson *et al.*<sup>25</sup> Acceptable fits to the data of these experiments can be obtained for any reasonable choice of  $\sigma_\rho$  or  $\alpha_\rho$  by suitable choice of the other.

(b)  $\gamma_\rho^2/4\pi$  is determined well if the  $\rho^0$  width and  $\sigma_\rho$  are given and DESY-MIT and Cornell agree here.

(c) The deuteron is important to constrain the normalization and helps to sharpen up the  $\chi^2$  maps. If one had complete confidence in the theory, a deuteron measurement combined with the massive

TABLE VI. Fixed- $\sigma_\rho$   $A$ -dependence fits for DESY-MIT.

$\sigma_\rho$ (mb)	23	24	25	26	27	28
$k = 5.8$ GeV						
$-\alpha_\rho$	$0.36 \pm 0.04$	$0.32 \pm 0.04$	$0.28 \pm 0.04$	$0.24 \pm 0.04$	$0.20 \pm 0.04$	$0.17 \pm 0.04$
$\chi^2_\rho$	72.3	71.5	70.6	70.2	69.7	69.4
$ f_0 ^2$ ( $\mu\text{b}/\text{GeV}^2$ )	105	107	109	111	112	114
$\gamma_\rho^2/4\pi$	0.53	0.55	0.58	0.60	0.63	0.66
$k = 6.2$ GeV						
$-\alpha_\rho$	$0.39 \pm 0.03$	$0.35 \pm 0.03$	$0.31 \pm 0.03$	$0.27 \pm 0.03$	$0.23 \pm 0.03$	$0.19 \pm 0.03$
$\chi^2_\rho$	62.4	60.5	59.2	58.2	57.5	57.2
$ f_0 ^2$ ( $\mu\text{b}/\text{GeV}^2$ )	110	112	114	116	118	119
$\gamma_\rho^2/4\pi$	0.52	0.54	0.56	0.58	0.61	0.64
$k = 6.6$ GeV						
$-\alpha_\rho$	$0.34 \pm 0.03$	$0.29 \pm 0.03$	$0.25 \pm 0.03$	$0.21 \pm 0.03$	$0.17 \pm 0.03$	$0.13 \pm 0.03$
$\chi^2_\rho$	60.5	58.7	57.3	56.3	55.8	55.5
$ f_0 ^2$ ( $\mu\text{b}/\text{GeV}^2$ )	103	105	107	108	110	112
$\gamma_\rho^2/4\pi$	0.54	0.56	0.58	0.61	0.64	0.66
$\sigma_\rho$ (mb)	29	30	31	32	33	
$k = 5.8$ GeV						
$-\alpha_\rho$	$0.04 \pm 0.04$	$0.10 \pm 0.04$	$0.072 \pm 0.04$	$0.038 \pm 0.04$	$0.009 \pm 0.04$	
$\chi^2_\rho$	69.3	69.3	69.3	69.4	69.6	
$ f_0 ^2$ ( $\mu\text{b}/\text{GeV}^2$ )	116	117	119	120	123	
$\gamma_\rho^2/4\pi$	0.69	0.72	0.76	0.79	0.83	
$k = 6.2$ GeV						
$-\alpha_\rho$	$0.16 \pm 0.03$	$0.12 \pm 0.03$	$0.091 \pm 0.03$	$0.058 \pm 0.03$	$0.026 \pm 0.03$	
$\chi^2_\rho$	57.2	57.6	58.0	58.9	60.0	
$ f_0 ^2$ ( $\mu\text{b}/\text{GeV}^2$ )	121	123	125	127	129	
$\gamma_\rho^2/4\pi$	0.66	0.69	0.72	0.75	0.79	
$k = 6.6$ GeV						
$-\alpha_\rho$	$0.10 \pm 0.03$	$0.06 \pm 0.03$	$0.025 \pm 0.03$	$-0.006 \pm 0.03$	$-0.03 \pm 0.03$	
$\chi^2_\rho$	55.6	56.1	57.0	58.4	60.5	
$ f_0 ^2$ ( $\mu\text{b}/\text{GeV}^2$ )	114	116	118	120	122	
$\gamma_\rho^2/4\pi$	0.70	0.73	0.76	0.80	0.83	

DESY-MIT data matrix would yield very-well-determined values of  $\sigma_\rho$  and  $\alpha_\rho$  as illustrated in Fig. 6.

#### V. MODEL DEPENDENCE OF THE RESULTS

In order to visualize the effect of small changes in the model, and also to compare results of different experiments, we have adopted the idea of normalizing to a standard reference cross section. That is, we divide the experimental or theoretical cross section by the reference cross section and plot the result vs  $A$ . This takes out the gross dependence on  $A$  and permits us to see systematic trends in the data. Experimentalists have used a similar procedure in presenting their data when they divide their cross sections by  $A^{3/2}$ . The factor  $A^{3/2}$  has no theoretical significance; it was

simply found to give roughly the over-all change in magnitude in the cross section between small and large  $A$ . We want, of course, to use a reference cross section which is reasonably close to the actual data. We will concentrate for the present on the Cornell data at 6.5 GeV and the DESY-MIT data at 6.6 GeV. The parameters for the reference cross section, which were selected before the data analysis was actually complete, are

$$\sigma_\rho = 27.5 \text{ mb,}$$

$$\alpha_\rho = -0.2,$$

$$|f_0|^2 = 117 \mu\text{b}/\text{GeV}^2 \text{ or } \gamma_\rho^2/4\pi = 0.63.$$

These do give forward cross sections reasonably close to the data, as can be seen from Fig. 8. This figure also shows that the two sets of experi-

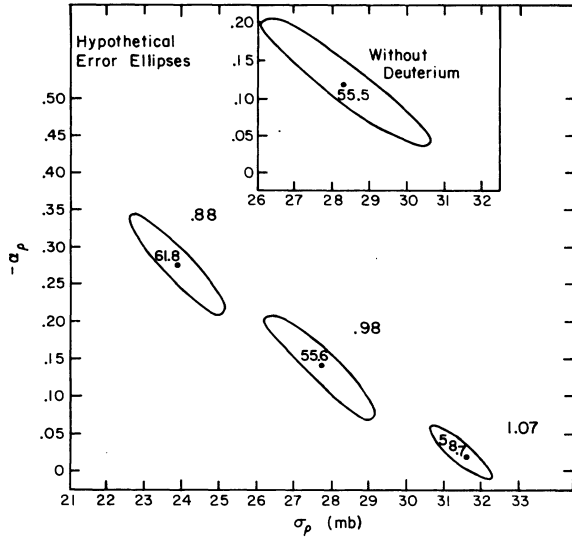


FIG. 6. Possible effect of a deuterium measurement on the DESY-MIT 6.6-GeV data. The number outside of each error ellipse is the fraction of the Cornell 6.5-GeV forward deuteron cross section assumed for the normalization of the hypothetical deuterium data.

mental data are in reasonable agreement with each other. Incidentally, the use of a reference cross section permits us to make a fairer comparison of the data since it "takes out" a variation of order (0.5–1.7)% (from small  $A$  to large  $A$ ) associated with the slightly different energies of the experiments. We see that the two sets of data differ more in normalization than in  $A$  dependence.

As described in Sec. IV, we were most interested in analyzing the data to obtain the values of  $\sigma_\rho$ ,  $\alpha_\rho$ , and  $|f_0|^2$ , rather than the nuclear parameters. We also studied (not very exhaustively) the claims of the DESY-MIT group that the  $t$  de-

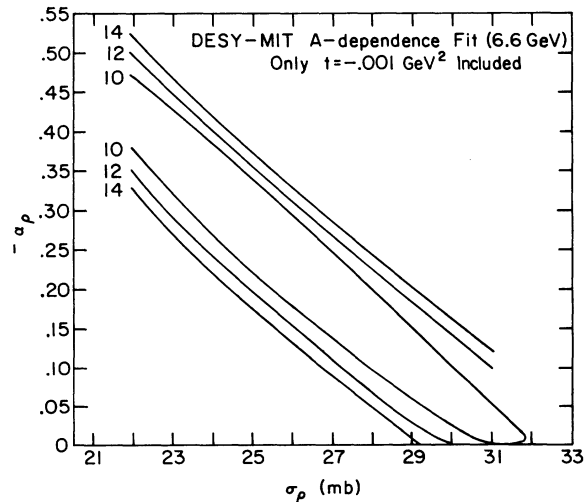


FIG. 7.  $\chi^2$  map for DESY-MIT at 6.6 GeV using only  $-t = 0.001 \text{ GeV}^2$  data.  $\langle \chi^2 \rangle = 10$ .

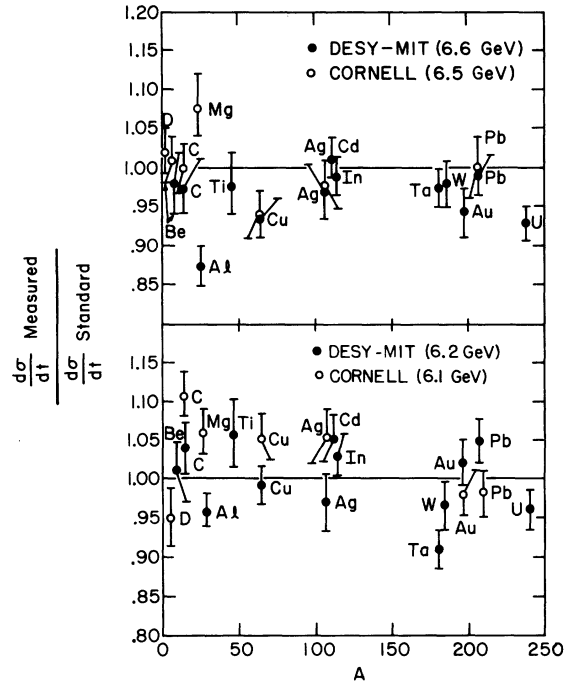


FIG. 8. Ratio of forward cross sections for DESY-MIT (Cornell) at 6.6, 6.2 (6.5, 6.1) GeV to theoretical forward cross sections calculated with the "standard" parameters (see text).

pendence of their data could be used to determine an accurate value of the nuclear radius. The present section will be concerned mainly with the effects of varying the different parameters by small amounts.

TABLE VII. Fixed- $\alpha_\rho$   $A$ -dependence fits for Cornell. The errors are included only for comparison with older analyses. They are for fixed  $\alpha_\rho$  and are misleadingly small, since these experiments do not determine either  $\sigma_\rho$  or  $\alpha_\rho$  uniquely.

	$\alpha_\rho = 0$	$\alpha_\rho = -0.2$	$\alpha_\rho = -0.3$
$k = 6.1 \text{ GeV}$			
$\sigma_\rho$ (mb)	$32.2 \pm 1$	$28.2 \pm 0.9$	$26.3 \pm 0.8$
$\chi^2$	21.1	12.4	9.0
$ f_0 ^2$ ( $\mu\text{b}/\text{GeV}^2$ )	$124 \pm 3\%$	$120 \pm 3\%$	$118 \pm 3\%$
$\gamma_\rho^2/4\pi$	$0.78 \pm 4\%$	$0.64 \pm 4\%$	$0.59 \pm 4\%$
$k = 6.5 \text{ GeV}$			
$\sigma_\rho$ (mb)	$32.9 \pm 1.4$	$29.6 \pm 1.3$	$27.8 \pm 1.2$
$\chi^2$	3.4	4.6	5.9
$ f_0 ^2$ ( $\mu\text{b}/\text{GeV}^2$ )	$123 \pm 3\%$	$120 \pm 4\%$	$119 \pm 3\%$
$\gamma_\rho^2/4\pi$	$0.82 \pm 6\%$	$0.70 \pm 6\%$	$0.66 \pm 6\%$
$k = 8.8 \text{ GeV}$			
$\sigma_\rho$ (mb)	$28.3 \pm 0.7$	$25.9 \pm 0.6$	$24.7 \pm 0.6$
$\chi^2$	22.1	17.5	15.9
$ f_0 ^2$ ( $\mu\text{b}/\text{GeV}^2$ )	$105 \pm 2\%$	$103 \pm 2\%$	$102 \pm 2\%$
$\gamma_\rho^2/4\pi$	$0.71 \pm 3\%$	$0.63 \pm 3\%$	$0.61 \pm 3\%$

TABLE VIII. Fixed- $\alpha_\rho$   $A$ -dependence fits for DESY-MIT. The same comment applies as in Table VII.

	$\alpha_\rho = 0$	$\alpha_\rho = -0.2$	$\alpha_\rho = -0.3$
$k = 5.8$ GeV			
$\sigma_\rho$ (mb)	$33.0 \pm 1.2$	$27.3 \pm 1$	$24.8 \pm 0.9$
$\chi^2$	69.7	69.6	70.9
$ f_0 ^2$ ( $\mu\text{b}/\text{GeV}^2$ )	$122 \pm 4\%$	$113 \pm 3\%$	$109 \pm 3\%$
$\gamma_\rho^2/4\pi$	$0.83 \pm 4\%$	$0.64 \pm 4\%$	$0.57 \pm 4\%$
$k = 6.2$ GeV			
$\sigma_\rho$ (mb)	$33.3 \pm 0.9$	$27.9 \pm 0.7$	$25.4 \pm 0.6$
$\chi^2$	60.7	57.3	58.8
$ f_0 ^2$ ( $\mu\text{b}/\text{GeV}^2$ )	$128 \pm 3\%$	$119 \pm 2\%$	$115 \pm 2\%$
$\gamma_\rho^2/4\pi$	$0.80 \pm 3\%$	$0.63 \pm 3\%$	$0.57 \pm 3\%$
$k = 6.6$ GeV			
$\sigma_\rho$ (mb)	$31.3 \pm 0.9$	$26.5 \pm 0.7$	$24.2 \pm 0.6$
$\chi^2$	57.7	56.0	58.6
$ f_0 ^2$ ( $\mu\text{b}/\text{GeV}^2$ )	$117 \pm 3\%$	$110 \pm 3\%$	$106 \pm 3\%$
$\gamma_\rho^2/4\pi$	$0.78 \pm 3\%$	$0.62 \pm 3\%$	$0.56 \pm 3\%$

$\sigma_\rho$ . Figure 9 shows the effect of changing  $\sigma_\rho$  while holding all the other parameters fixed. Since  $\sigma_\rho$  yields the absorption of the  $\rho$  meson on the way out of the nucleus, it is not surprising that increasing  $\sigma_\rho$  decreases the cross section by an amount which is relatively more important for heavy nuclei. Since the gross normalization effect due to increasing  $\sigma_\rho$  could be compensated by a change in  $|f_0|^2$ , it is important to look primarily at the systematic  $A$  dependence in studying these curves. (Note: If we were holding  $\gamma_\rho^2/4\pi$  fixed,  $|f_0|^2$  would increase with  $\sigma_\rho$  in such a way that  $\gamma_\rho^2/4\pi$  would have to be increased to restore over-all normalization.)

$\alpha_\rho$ . As first pointed out by Swartz and Talman,<sup>11</sup> changes in  $\sigma_\rho$  can be compensated for (aside from over-all normalization) by appropriate changes in  $\alpha_\rho$ . This can be understood from a study of Fig. 9. To the extent that changes in the cross section are roughly linear in  $\Delta\alpha_\rho$  and  $\Delta\sigma_\rho$ , we would expect that an increase in  $\sigma_\rho$  of about 2 mb would be compensated for by an increase in  $\alpha_\rho$  of about 0.1, if at the same time  $|f_0|^2$  were increased by about 3% (this corresponds to increasing  $\gamma_\rho^2/4\pi$  if VMD is assumed). It is now clear that by taking an appropriate combination of changes in  $\sigma_\rho$  and  $\alpha_\rho$ , one can obtain an  $A$  dependence which is nearly the same as that of the reference cross section. It is for this reason that the  $\chi^2$  map tends to have long valleys in which  $\chi^2$  changes only slowly along the valley. It should be emphasized that the previous discussion applies to nuclei excluding the deuteron. The cross section for deuterium depends more on  $|f_0|^2$  than the other parameters, and it can therefore help in limiting the fit to the

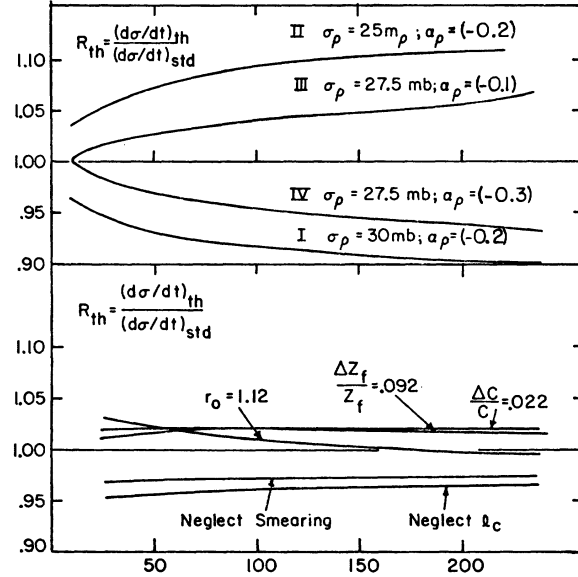


FIG. 9. Effect of changing various  $\rho^0$  and nuclear parameters on the  $A$  dependence of the optical model.

data, as was explained in Sec. IV.

$m_\rho$ . Changing the  $\rho^0$  mass of the optical model changes the longitudinal momentum transfer, and the phase factor this introduces is only important in heavy nuclei. If the mass is changed by 10 MeV, the cross section changes by 3% in Pb, so this is a very small effect.

*Nuclear parameters.* Figure 9 shows the effect of varying the nuclear radius, surface thickness, and omitting any one of the smearing effects or correlation effects. Whatever  $A$  dependence each of these effects gives could result in a change in the parameters of interest  $\sigma_\rho$  and  $\alpha_\rho$ , as can be estimated by comparison with Fig. 9.<sup>26</sup> It should be remarked that we are displaying here the dependence of the forward cross section on these parameters. The analysis of the DESY-MIT data involves fitting the  $t$  dependence over a significant range, so this display could be somewhat misleading. We try to allow for this by comparing our approach with the DESY-MIT approach to fitting the nuclear radii.

*Corrections of order  $A^{-1}$ .* The optical model is derived from multiple-scattering theory under the assumption that  $A \gg 1$ . This permits the exponentiation of products of factors  $(1-\beta)$  where  $\beta \ll 1$ . The error made in replacing a product of factors by an exponential is called a "1/A correction."<sup>27</sup> This correction is most apparent in the independent-particle approximation. However, it can be shown that the correction is partially compensated in the treatment of two-body correlations.<sup>28</sup> A more general discussion can be given with the conclusion, barring important collective

effects, that the corrections should be extremely small for any of the nuclei considered here. Accordingly, we feel that it is quite well justified to use the exponentiated form of the optical model.

We have made a not-very-exhaustive study of the use of the DESY-MIT data to determine the nuclear radii. In their analysis, the effects of smearing and correlation were neglected, and the surface thickness was held fixed ( $z_F=0.545 F$ ), while the nuclear radius  $c$  was varied. The Fermi shape was used for all nuclei, including the light ones. We do not criticize their neglect of smearing and correlations. They are determining, in effect, an optical density directly, while we are basing our analysis on some assumed properties of nuclei.

In this sort of an analysis, there are many possible variants of the same basic model, and an exploration of their detailed idiosyncrasies would be neither interesting nor productive. Therefore we restrict ourselves to two models, with fixed  $\sigma_\rho$  ( $=27.5$  mb) and  $\alpha_\rho$  ( $=-0.2$ ). These are the model used by the DESY-MIT group and the model used in this paper. We use the "stable"  $\rho^0$  cross sections. That is, we first analyze the mass dependence at fixed  $k$  and  $t$  to determine the  $\rho^0$  cross section, as has been discussed in another section. In contrast, the DESY-MIT group have made a radius fit to each mass bin at fixed  $k$ . Since we do not feel secure in our understanding of the  $\rho^0$  mass shape, we prefer our approach; but the final agreement of our results with theirs (within errors) is an indication that the precise details are not too important. In carrying out the fit to the  $t$  dependence, the normalization ( $|f_0|^2$ ) was left free for each nucleus at each energy. Any systematic variation of  $|f_0|^2$  with  $A$  is then to be

attributed to  $\sigma_\rho$  or  $\alpha_\rho$ . Variation of  $z_F$  with  $A$  can be compensated by the  $A$  dependence of  $c$ . In their more exhaustive study, the DESY-MIT group conclude that the most important parameter in the analysis is  $\langle r^2 \rangle$ , rather than  $c$  and  $z_F$  separately.

The results are shown in Table IX for those nuclei which are assumed to have a Fermi shape ( $A > 16$ ). Generally we confirm that for a specific nuclear model, the DESY-MIT data can be used to obtain a very good value for the radius. Our results, using their nuclear model, agree quite well with theirs. In some cases, our errors are larger than theirs because we used too few points in the  $t$  distribution. In the model with smearing and correlation effects included, the radii are slightly smaller, and do not disagree unreasonably with the values used in our analysis of the data.

In summary, we agree with the conclusion of the DESY-MIT group that their data can be used to obtain quite accurate values of the nuclear radius providing other features of the model (smearing, correlations,  $\sigma_\rho$ ,  $\alpha_\rho$ ,  $z_F$ , etc.) are held fixed. The dependence on these other parameters is actually rather small, and the changes in  $c$  due to variations in  $z_F$ ,  $r_{em}$ , and  $r_s$  correspond mostly to keeping  $\langle r^2 \rangle$  fixed.

*Corrections from incoherent production.* We have all but ignored the effects of incoherent production of  $\rho^0$  mesons. Our principal justifications are that this correction is expected to be rather small in any case and further that the existing theoretical treatments are probably not sufficiently precise to be quantitatively reliable in the very-small- $t$  region. Thus it seemed best to indicate that there are uncertainties from this cause rather than to imply that they have been properly taken into account. In the Born approximation, the near-

TABLE IX. A comparison of the best-fit radii of DESY-MIT with our best-fit radii obtained by two methods: using our best approximation to the DESY-MIT nuclear model and using our own nuclear model.

	Our fit, our model <sup>a</sup>	Our fit, "DESY-MIT model" <sup>b</sup>	DESY-MIT best fit <sup>c</sup>
U	1.09 ± 0.02	1.10 ± 0.02	1.11 ± 0.02
Pb	1.15 ± 0.03	1.16 ± 0.03	1.15 ± 0.03
Au	1.11 ± 0.03	1.12 ± 0.03	1.11 ± 0.05
W	1.07 ± 0.03	1.08 ± 0.03	1.11 ± 0.02
Ta	1.08 ± 0.03	1.09 ± 0.03	1.15 ± 0.03
In	1.11 ± 0.03	1.12 ± 0.03	1.15 ± 0.05
Cd	1.15 ± 0.03	1.16 ± 0.03	1.12 ± 0.03
Cu	1.05 ± 0.05	1.07 ± 0.05	1.14 ± 0.03

<sup>a</sup> Our nuclear model (see Sec. II) includes two-body correlations and "smearing" to take into account the finite range of the two-body interactions. But no incoherent background is subtracted from the data.

<sup>b</sup> Same model without correlations or smearing. This is our best approximation to the DESY model without making a background subtraction.

<sup>c</sup> 6.54-GeV best-value radii taken from Table I of Ref. 12. The number shown is  $c/A^{1/3}$ .

forward incoherent production would be rather small because of the small momentum transfer. However, when multiple scattering is taken into account, refraction and absorption can give an over-all coherent momentum transfer which can supply the momentum transfer necessary to excite a single nucleon. Our treatment entirely ignores the possible suppression in the cross section from the orthogonality of the excited states to the ground state; therefore, we expect it to be an overestimate, which is particularly bad for light nuclei where multiple-scattering effects are less important.

Estimates of incoherent production using the independent-particle model have been made by Trefil.<sup>21</sup> They do show such a strong suppression for light nuclei, but only a small one for heavy nuclei. Unfortunately, the independent particle model does not properly take into account exclusion principle effects, which would be expected to further reduce the incoherent contribution. An indication of this appears in a calculation by Czyż *et al.*,<sup>29</sup> who evaluated incoherent proton scattering from  $O^{16}$  on various assumptions. Reading from their curve, the independent-particle model results in a reduction by a factor of about 2, while the use of antisymmetric wave functions gives a factor of about 3. We know of no similar results for heavy nuclei.

The theory of near-forward incoherent production ( $-t \lesssim 0.01$ ) is very subtle because it requires a precise knowledge of the two-particle correlation function. Around each particle is a "hole" in which one particle is missing from the total number of particles in the nucleus. It is the interference term between production amplitudes from the particle and the hole which tends to reduce the cross section. In the independent particle model, this hole is spread over the whole nucleus, and the interference is consequently rather small compared to the direct term. In a more realistic model including the exclusion principle, the hole would

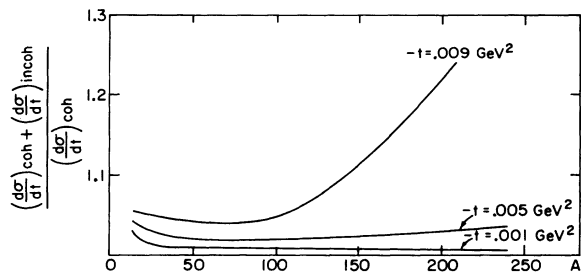


FIG. 10. Effect on the  $A$  dependence of adding "half-strength" incoherent corrections to the coherent optical-model calculations. Curves for three different values of  $t$  are shown.

be much more localized and the compensation would be more complete (in the limit where the hole is a  $\delta$  function, the two amplitudes cancel exactly). Because most of the incoherent production comes from large impact parameters where correlations are poorly understood, a believable analysis of the effect has yet to be made.

Figure 10 illustrates the possible effect of incoherent production on the interpretation of the experiment. Since we believe the suppression is likely to be at least a factor of 2, "half incoherent" is used as a realistic estimate of the upper limit of the incoherent background. For small  $t$ , the effect is greater in the light nuclei; of course, this may be misleading since the incoherent cross section is probably suppressed more for lighter nuclei. Since the coherent production decreases with increasing  $|t|$ , the incoherent production becomes relatively more important at larger  $|t|$  and it ultimately dominates the cross section. For obvious reasons, this happens at smaller  $|t|$  for larger nuclei. From this figure, it seems clear that while incoherent production might cause a small quantitative change in the fit, it should not change the qualitative picture. This is borne out by the analysis of Sec. IV; see Fig. 2.

## VI. SUMMARY AND CONCLUSIONS

Although the theory is not sufficiently well understood to enable us to determine  $\sigma_p$  and  $\alpha_p$  completely from these experiments, our analysis shows that if one is known, the other is well determined. For these experiments the relationships between  $\sigma_p$  and  $\alpha_p$  is roughly independent of energy and can be very crudely given as  $\sigma_p(\alpha_p) = 32 + \alpha_p / 0.05$  mb. The model dependence of these conclusions was described extensively in Sec. V. (Here we note only that different model assumptions do not change the conclusions qualitatively, and make rather small quantitative changes.)

Directing the reader's attention to Tables VII, VIII, and X, we note that our results are in excellent agreement with the older analyses of Refs. 2 and 3. In this connection we note some important points:

(1) The DESY-MIT analysis was done with  $\alpha_p$  fixed at  $-0.2$ . Cornell used different values of  $\alpha_p$  at each energy (see Ref. 3).

(2) The nuclear radii used by the two groups differ from our radii of Tables I and II. For a discussion of this effect, see Sec. V.

(3) Our errors on  $|f_0|^2$  and  $\gamma_p^2/4\pi$  in Tables VII and VIII are considerably smaller than in the older analyses. This may be due to our arbitrary choice,  $\Gamma_p = 127$  MeV, which we take to be an ex-

TABLE X. Results of the fixed- $\alpha_\rho$  analyses made by the Cornell and DESY-MIT groups themselves. Taken from Refs. 2 and 3.

Cornell <sup>a</sup>					
$k$ (GeV)	Nuclear parameters <sup>a</sup>	$\alpha_\rho$	$\gamma_\rho^2/4\pi$	$\sigma_\rho$ (mb)	$ f_0 ^2$ ( $\mu\text{b}/\text{GeV}^2$ )
8.8	Best fit	-0.24	$0.68 \pm 0.04$	$26.8 \pm 1.2$	$105 \pm 11$
	E-S	-0.24	$0.63 \pm 0.04$	$25.9 \pm 1.0$	$106 \pm 11$
6.5	Best fit	-0.27	$0.74 \pm 0.04$	$30.1 \pm 1.5$	$124 \pm 15$
	E-S	-0.27	$0.65 \pm 0.05$	$27.9 \pm 1.3$	$120 \pm 15$
6.1	Best fit	-0.27	$0.58 \pm 0.03$	$26.1 \pm 0.9$	$117 \pm 10$
	E-S	-0.27	$0.62 \pm 0.04$	$27.5 \pm 1.1$	$122 \pm 13$
DESY-MIT <sup>b</sup>					
$\sigma_\rho = 26.7 \pm 2$ mb, $\alpha_\rho = -0.2$					
$ f_0 ^2 = 118 \pm 6$ $\mu\text{b}/\text{GeV}^2$ , $\gamma_\rho^2/4\pi = 0.57 \pm 0.1$					

<sup>a</sup> Cornell presents results for two different sets of nuclear parameters. The "best fit" parameters come from optical-model analyses of proton-nucleus and neutron-nucleus total cross sections. The "E-S" parameters come from electron scattering experiments. See Ref. 3 and references cited therein for further details. In general, our nuclear radii are closer to the E-S radii, although we keep  $z_F$  fixed at 0.545 F throughout.

<sup>b</sup> DESY-MIT presents results for several different assumed forms for the  $\pi\pi$  mass distributions. Here we give the sample result chosen by them in Ref. 2.

actly given number. (Our results for  $|f_0|^2$  and  $4\pi/\gamma_\rho^2$  are proportional to this choice.) In any event, since we cannot determine  $\sigma_\rho$  or  $\alpha_\rho$  uniquely, there is little point in giving errors for  $|f_0|^2$  or  $\gamma_\rho^2/4\pi$ , quantities which depend strongly on  $\sigma_\rho$  and  $\alpha_\rho$ . The errors given in Tables VII and VIII are for fixed  $\alpha_\rho$ , and are misleading in their smallness. They are included only to facilitate comparison with the older analyses.

(4) Our agreement with the DESY-MIT value of  $\gamma_\rho^2/4\pi$  may appear to be a little better than it actually is because of compensating differences in the models used. Our standard width of 127 MeV should have led to a smaller experimental cross section (hence larger  $\gamma_\rho^2/4\pi$ ) than their analysis, which was based on a width of 140 MeV. On the other hand, we did not make any background subtraction since we felt the theory of the  $\rho^0$  shape was too unreliable. It is our position that only the noncoherent pion-pair background should be subtracted. Coherent, but nonresonant, pion pairs should be considered a part of the Drell amplitude, and their effect should be canceled out at the  $\rho^0$  mass, as pointed out by Bauer<sup>18</sup> and Pumplin<sup>19</sup> and discussed in the accompanying article.<sup>7</sup> Nevertheless, this serves to emphasize that there is considerable uncertainty in the overall normalization of the data which is very hard to assess. There is no reason to suppose, however, that this gives a significant  $A$ -dependent effect.

(5) We have not made a detailed comparison with the original analysis the Cornell group made of their data, in which they did not introduce a real

part. We agree qualitatively in that this gives large values of  $\sigma_\rho$  and  $\gamma_\rho^2/4\pi$ , but have not tried to reproduce their model precisely.

Both experiments yield approximately the same relationship between  $\sigma_\rho$  and  $\alpha_\rho$  but their results are slightly different (see Sec. IV). In particular, Cornell's deuterium measurement tied down their value of  $|f_0|^2$  so that it varied much less with  $\sigma_\rho$  (or  $\alpha_\rho$ ) than the  $|f_0|^2$  for DESY-MIT. Equally important is the DESY-MIT  $t$  dependence which gave them much better statistics than Cornell and kept the  $\chi^2$  minimum from fluctuating very much from energy to energy, as it does in the Cornell case. When these special features are removed, i.e., the Cornell deuterium measurement and the DESY-MIT  $t$  dependence, the two experiments agree completely—although very little information then remains in the resulting flat  $\chi^2$  valleys (see Sec. IV). In effect, because of our lack of confidence in the precise positions of  $\chi^2$  minima, the two experiments yield comparable information. If one had complete confidence in the theory, however, a deuterium measurement by DESY-MIT would have made a rather good determination of  $\sigma_\rho$  and  $\alpha_\rho$  possible (see Sec. IV). Nevertheless, we would not encourage further  $\rho^0$  photoproduction experiments until significant theoretical advances are made, particularly in the area of incoherent background subtractions.

As a final note, we point out that our value of  $|f_0|^2$  from the fixed- $\alpha_\rho$  fits to the Cornell 8.8-GeV data,  $103 \mu\text{b}/\text{GeV}^2 \pm 2\%$ , is in excellent agreement with a later Cornell experiment on  $\rho^0$  photoproduction at 8.5 GeV from hydrogen.<sup>30</sup> In that experiment the recoil proton was detected to eliminate the inelastic background. Hydrogen data have also been presented in Refs. 2 and 3 and again our fixed- $\alpha_\rho$  fits are in reasonable agreement with the hydrogen values of  $|f_0|^2$  as given there. Although those experiments did not correct for inelastic background, the general agreement between the hydrogen and complex nuclei values of  $|f_0|^2$  may indicate that the inelastic background is not too important.

#### ACKNOWLEDGMENTS

We are indebted to both the DESY-MIT and Cornell groups for important information and very helpful discussions. Dr. U. Becker, Dr. N. Mistry, Professor A. Silverman, Professor S. Ting, and, especially, Professor R. Talman deserve special thanks. We have also enjoyed the constant support and advice of Professor F. Pipkin and Professor K. Gottfried, with whom we are preparing a review article on hadronic photon interactions. One



of us (D. R. Y.) wishes to thank Professor S. Drell for his hospitality at SLAC where part of this work was organized, and his colleagues there, particu-

larly Dr. S. Brodsky, Professor D. Leith, and Dr. L. Stodolsky, for many useful discussions.

\*Work supported in part by the National Science Foundation.

<sup>1</sup>A good overview of vector-meson dominance is given by J. J. Sakurai in *Proceedings of the Fourth International Symposium on Electron and Photon Interactions at High Energies*, edited by D. W. Braben (Daresbury Nuclear Physics Laboratory, Daresbury near Warrington, Lancashire, England, 1969). A review emphasizing the role of vector-meson dominance in photonic processes is given by K. Gottfried in *Proceedings of the 1971 International Symposium on Electron and Photon Interactions at High Energies*, edited by N. B. Mistry (Laboratory of Nuclear Studies, Cornell University, Ithaca, New York, 1972).

<sup>2</sup>H. Alvensleben *et al.*, Nucl. Phys. **B18**, 333 (1970).

<sup>3</sup>G. McClellan *et al.*, Phys. Rev. D **4**, 2683 (1971).

<sup>4</sup>The original experiment for this process is L. J. Lanzerotti *et al.*, Phys. Rev. **166**, 1365 (1968). Other recent measurements of  $\rho^0$  photoproduction on complex nuclei include F. Bulos *et al.* [Phys. Rev. Lett. **22**, 490 (1969)], and H. J. Behrend *et al.* [Phys. Rev. Lett. **24**, 336 (1970)]. We discuss the data of Refs. 2 and 3 exclusively, however, since they are both the most comprehensive and the most easily analyzed by our procedures.

<sup>5</sup>S. D. Drell and J. S. Trefil, Phys. Rev. Lett. **16**, 552 (1966); **16**, 832(E) (1966).

<sup>6</sup>M. Ross and L. Stodolsky, Phys. Rev. **149**, 1172 (1966).

<sup>7</sup>R. Spital and D. R. Yennie, preceding paper, Phys. Rev. D **9**, 126 (1974).

<sup>8</sup>R. J. Glauber, in *Lectures in Theoretical Physics*, edited by W. E. Britten and L. G. Dunham (Interscience, New York, 1959), Vol. 1; in *High Energy Physics and Nuclear Structure*, edited by S. Devons (Plenum, New York, 1970), and references cited therein.

<sup>9</sup>K. Gottfried and D. R. Yennie, Phys. Rev. **182**, 1595 (1969).

<sup>10</sup>K. S. Kolbig and B. Margolis, Nucl. Phys. **B6**, 85 (1968); N. Jurisic, Ph.D. thesis, Cornell University, 1970 (unpublished); D. R. Yennie, in *Hadronic Interactions of Electrons and Photons* (Academic, London, 1971); E. J. Moniz and G. D. Nixon, Ann. Phys. (N.Y.) **67**, 58 (1971).

<sup>11</sup>J. Swartz and R. Talman, Phys. Rev. Lett. **23**, 1078 (1969).

<sup>12</sup>H. Alvensleben *et al.*, Phys. Rev. Lett. **24**, 792 (1970).

<sup>13</sup>Let the photoproduction amplitudes for the proton and the neutron be  $f_p = f_0 + f_1$  and  $f_n = f_0 - f_1$ , respectively. Then for a given nucleus we have  $f_0(A) = (Zf_p + Nf_n)/A = f_0 + (Z - N)f_1/A$ . Our approximation is that  $f_0(A) = f_0$ , which introduces an additional spurious  $A$  dependence into our analysis. We can estimate this effect using VMD to relate the photoproduction amplitudes to the total  $\gamma p$  and  $\gamma n$  cross sections:  $\sigma_{\gamma p}^{\text{tot}} \propto f_0 + 2f_1$ ,  $\sigma_{\gamma n}^{\text{tot}} \propto f_0 - 2f_1$ , where the factor of 2 enters because both  $\rho$ -to- $\omega$  and  $\omega$ -to- $\rho$  transitions are present in the total cross sections. Using experimental values for

$\sigma_{\gamma p}^{\text{tot}}$  and  $\sigma_{\gamma n}^{\text{tot}}$  at 6 GeV, we find  $f_1/f_0 \approx 2\%$ . The maximum value of  $|(Z - N)/A| \lesssim \frac{1}{5}$ , so that this effect introduces a normalization error that varies by  $<1\%$  across the periodic table. This is clearly negligible compared to other uncertainties of the model discussed in Sec. V. However, in the case of photoproduction of  $\omega^0$ , the photon couplings enter differently and the net effect is to make  $f_1/f_0$  for the  $\omega^0$  roughly  $9(f_1/f_0)$  for the  $\rho^0$ . Thus a 1% effect for the  $\rho^0$  may be a 9% effect for the  $\omega^0$ .

<sup>14</sup>J. Heisenberg *et al.*, Phys. Rev. Lett. **23**, 1402 (1969).

<sup>15</sup>We thank Professor K. Gottfried for supplying us with a value for the correlation length. He used the two-body correlation function of Moniz and Nixon (Ref. 10) and took into account the finite range of the two-body interactions. Without this finite-range correction, first pointed out by von Bochmann *et al.* (Ref. 16), the correlation length would have been of order 0.75 F. See Ref. 26 for a brief discussion of how the correlation length affects the results quantitatively.

<sup>16</sup>G. von Bochmann, B. Margolis, and C. L. Tang, Phys. Lett. **30B**, 254 (1969).

<sup>17</sup>K. Gottfried and D. Julius, Phys. Rev. D **1**, 140 (1970).

<sup>18</sup>T. H. Bauer, Phys. Rev. D **3**, 2671 (1971).

<sup>19</sup>J. Pumplin, Phys. Rev. D **2**, 1859 (1970).

<sup>20</sup>H. Alvensleben *et al.*, Phys. Rev. Lett. **27**, 888 (1971).

<sup>21</sup>J. S. Trefil, Nucl. Phys. **B11**, 330 (1969).

<sup>22</sup>C. R. Schumacher, private communication. For small  $\vec{q}^2$ ,

$$F_d(\vec{q}^2) \equiv \int e^{-i\vec{q} \cdot \vec{r}} |\phi_{\text{grnd}}^d(\vec{r})|^2 d^3r = 1 - \frac{2}{3} \vec{q}^2 (3.86),$$

where  $\vec{q}^2$  is in inverse-square fermis, and  $\phi_{\text{grnd}}^d(\vec{r})$  is the deuteron ground-state wave function.

<sup>23</sup>M. Damashek and F. J. Gilman, Phys. Rev. D **1**, 1319 (1970). These results have recently been confirmed experimentally at 2.2 GeV by H. Alvensleben *et al.*, Phys. Rev. Lett. **30**, 328 (1973).

<sup>24</sup>H. Alvensleben *et al.*, Phys. Rev. Lett. **25**, 1377 (1970); Nucl. Phys. **B25**, 342 (1971).

<sup>25</sup>R. Anderson *et al.*, Phys. Rev. D **4**, 3245 (1971).

<sup>26</sup>For example, consider the effect of neglecting  $l_c$ . This would change the  $A$  dependence by about 2%, which could be compensated for by increasing  $\sigma_\rho$  by  $\sim 1$  mb (or increasing  $-\alpha_\rho$  by  $\sim 0.05$ ). These two modifications would in turn lead to over-all normalization changes requiring an increase of about 7% in  $|f_0|^2$ . The resulting change in  $\gamma_\rho^2/4\pi$  would be negligible since the changes in  $\sigma_\rho$  and  $|f_0|^2$  compensate each other.

<sup>27</sup>Here  $\beta$  is proportional to the diameter of the nucleus, which varies like  $A^{1/3}$ , and also to the probability density of a single nucleon which varies like  $A^{-1}$ . Since it turns out that the apparent correction is of relative order  $\beta$ , the terminology " $A^{-1}$  correction" is misleading.

<sup>28</sup>See D. R. Yennie, Ref. 10, page 336, for a brief

discussion of this point.

<sup>29</sup>W. Czyż, L. Lesniak, and H. Wołek, Nucl. Phys. **B19**, 125 (1970); **B25**, 638 (1971). See also E. Błeszynska,

M. Błeszynski, A. Małecki, and P. Picchi, Phys. Lett. **43B**, 355 (1973).

<sup>30</sup>C. Berger *et al.*, Phys. Lett. **39B**, 659 (1972).

## Quark-parton fragmentation functions\*

Jean Cleymans†

*III. Physikalisches Institut, Technische Hochschule, Jägerstrasse, Aachen, Germany (F.R.)*

Rudolf Rodenberg‡

*Centro Brasileiro de Pesquisas Fisicas, Av. Wenceslau Braz, Rio de Janeiro, Brasil*

(Received 19 July 1973)

The distributions of  $\pi^+$  and  $\pi^-$  produced in the current fragmentation region are analysed in the framework of the quark-parton model. Motivated by experimental results on deep-inelastic neutrino scattering, we have neglected antiquark (and strange quark) contributions whenever the Bjorken scaling variable  $x$  is not close to zero. This approximation enables us to extract the quark fragmentation functions  $D_u^{\pi^+}(z)$  and  $D_d^{\pi^+}(z)$ . The  $\pi^+/\pi^-$  asymmetry is then calculated as a function of  $Q^2$ . This tests the factorization properties of the quark-parton model as a whole range of  $x$  values is involved. Agreement with existing data is found. Predictions for future experiments are also presented.

### I. INTRODUCTION

The quark-parton model together with the assumption of short-range correlations in rapidity space give a specific description for the distributions of hadrons produced either in current-hadron collisions or in electron-positron annihilation<sup>1-4</sup>. We want to analyze present data on  $\pi$  distributions in the current fragmentation region in  $e^- - p$  collisions. This provides a first test of the model and gives predictions for future experiments. The test relies heavily on the assumption that in the current fragmentation region the hadron distribution function factorizes into a part which depends only on the target particle and a second part which depends only on the emitted particle. We will first extract the quark-parton density functions from deep-inelastic lepton-hadron collisions.<sup>5</sup> As a second step we extract the parton fragmentation functions from data on  $e^- + p \rightarrow e^- + \pi + \text{anything}$  at a fixed value of  $x$  ( $=1/\omega$ ).<sup>6</sup> Combining these two pieces of information we can calculate the  $\pi^+/\pi^-$  ratio for increasing  $Q^2$  and compare with experimental data from SLAC.<sup>7</sup> Predictions for future experiments are also given. The next section is devoted to notations.

### II. NOTATIONS

We will study the hadron distributions as a function of the Feynman scaling variable  $z = p_z/p_{\max}$ ,

where  $p_z$  is the  $z$  component of the momentum of the final-state hadron in the current-proton center-of-mass frame, and  $p_{\max}$  is the maximal momentum a hadron in the final state can have. In the current fragmentation region  $z$  is positive.

Following Feynman,<sup>3</sup> we introduce the distributions  $N_{ep}(x, z)$  defined as

$$N_{ep}(x, z) = \frac{1}{\sigma_{\text{tot}}} \frac{d\sigma}{dz}. \quad (1)$$

The Lorentz-invariant inclusive cross section

$$F(z, p_T^2) = \frac{1}{\sigma_{\text{tot}}} \frac{E}{p_{\max}} \frac{d\sigma}{dz dp_T^2} \frac{1}{\pi} \quad (2)$$

has been parametrized in Ref. 6 as

$$F(z, p_T^2) = F(z, 0) e^{-B p_T^2}. \quad (3)$$

[We neglect the difference between the variable  $z$  and the variable  $x'$  introduced in Ref. 6. The dependence on  $\nu$  and  $Q^2$  has, for simplicity, not been indicated in (2) and (3)].  $B$  might be a function of  $\nu$  and  $Q^2$ . The relation between  $N$  and  $F$  is

$$N_{ep}(x, z) = \pi \frac{p_{\max}}{E} \int dp_T^2 F(z, p_T^2) \\ = \frac{\pi}{B} \frac{p_{\max}}{E} F(z, 0), \quad (4)$$

which in the parton fragmentation region (fast particles in the current fragmentation region) is